Open Access Articles

Formulation of the Sea Surface Friction Velocity in Terms of the Mean Wind and Bulk Stability

The Faculty of Oregon State University has made this article openly available.
Please share how this access benefits you. Your story matters.

Citation	Vickers, D., Mahrt, L., & Andreas, E. L. (2015). Formulation of the sea-surface friction velocity in terms of the mean wind and bulk stability. Journal of Applied Meteorology and Climatology, 54(3), 691-703. doi:10.1175/JAMC-D-14-0099.1
DOI	10.1175/JAMC-D-14-0099.1
Publisher	American Meteorological Society
Version	Version of Record
Terms of Use	http://cdss.library.oregonstate.edu/sa-termsofuse

Formulation of the Sea Surface Friction Velocity in Terms of the Mean Wind and Bulk Stability

DEAN VICKERS

Oregon State University, Corvallis, Oregon

LARRY MAHRT

Northwest Research Associates, Redmond, Washington

EDGAR L ANDREAS

Northwest Research Associates, Lebanon, New Hampshire

(Manuscript received 18 April 2014, in final form 14 November 2014)

ABSTRACT

Over 5000 aircraft eddy-covariance measurements from four different aircraft in nine different experiments are used to develop a simple model for the friction velocity over the sea. Unlike the widely used Coupled Ocean–Atmosphere Response Experiment (COARE) bulk flux scheme, the simple model (i) does not use Monin–Obukhov similarity theory (MOST) and therefore does not require an estimate of the Obukhov length, (ii) does not require a correction to the wind speed for height or stability, (iii) does not require an estimate of the aerodynamic roughness length, and (iv) does not require iteration. In comparing the model estimates developed in this work and those of the COARE algorithm, comparable fitting metrics for the two modeling schemes are found. That is, using Monin–Obukhov similarity theory and the Charnock relationship did not significantly improve the predictions. It is not clear how general the simple model proposed here is, but the same model with the same coefficients based on the combined dataset does a reasonable job of describing the datasets both individually and collectively. In addition, the simple model was generally able to predict the observed friction velocities for three independent datasets that were not used in tuning the model coefficients. Motivation for the simple model comes from the fact that physical interpretation of MOST can be ambiguous because of circular dependencies and self-correlation. Additional motivation comes from the large uncertainty associated with estimating the Obukhov length and, especially, the aerodynamic roughness length.

1. Introduction

Monin–Obukhov similarity theory (MOST) and the Charnock relationship are the basis for a large fraction of the air–sea bulk flux models embedded in general circulation models and mesoscale models in use today. Despite the widespread usage and apparent overall success, physical interpretation of MOST can be ambiguous because of circular dependencies and self-correlation (Hicks 1978; Kenney 1982; Andreas and Hicks 2002; Klipp and Mahrt 2004; Baas et al. 2006). MOST requires an iterative process to predict the turbulent momentum and heat fluxes in terms of transfer coefficients that depend on stability functions, which depend on the Obukhov length L, which itself depends on the turbulent fluxes of heat, moisture, and momentum, and so on. This is particularly problematic for stable stratification where relating the drag coefficient or the nondimensional shear to z/L (where z is height) leads to self-correlation that is the same sign as the expected physical correlation.

Over the sea, the ambiguity is compounded using the Charnock relationship (Charnock 1955), where the roughness length is specified to be a function of the surface stress, while the surface stress is specified to be a function of the roughness length. Such a circular feedback can lead

Corresponding author address: Dean Vickers, College of Earth, Ocean, and Atmospheric Sciences, Oregon State University, CEOAS Admin Bldg. 104, Corvallis, OR 97331.
E-mail: vickers@coas.oregonstate.edu

DOI: 10.1175/JAMC-D-14-0099.1

© 2015 American Meteorological Society

to extremely small estimates of the roughness length and to momentum fluxes that are less than smooth flow values (Mahrt et al. 2001).

Additional motivation for a simple model that does not rely on MOST is the large uncertainty associated with estimating the Obukhov length. Measurements of the friction velocity over the sea have minimum uncertainties estimated to be about 10% (Fairall et al. 1996), and the relative uncertainty increases with decreasing wind speed. Because determining the Obukhov length requires the friction velocity cubed, L may be uncertain by at least 30% (Andreas et al. 2012) without even considering the uncertainty in the heat and moisture fluxes. In weak winds less than about 4 m s^{-1}, additional uncertainty can arise as a result of the choice of analysis methods when evaluating the 10-m neutral equivalent drag coefficient C_{DN10}. Vickers et al. (2013) tested six unique processing schemes that involved different methods for averaging the surface stress and the wind speed and found striking differences in C_{DN10} at low wind speed. Significant additional uncertainty with the standard bulk flux model is associated with estimating the aerodynamic roughness length (e.g., Vickers and Mahrt 2010; Mahrt et al. 2001).

Here, we develop a formulation for the friction velocity that depends in a straightforward way on two fundamental characteristics of the mean flow known to influence the turbulence strength and the transfer of momentum: wind speed and bulk stability. The simple formulation does not use MOST, the Obukhov length, the Charnock relationship, or the aerodynamic roughness length and does not assume any special shape of the wind speed profile. We do not standardize the measured wind speed to a uniform height, say 10 m, because doing so would require introducing the quantity that we are estimating, friction velocity, into the independent variable, wind speed. This work represents a philosophical shift away from the drag coefficient and the roughness length because these are poorly behaved in weak winds (Mahrt et al. 2001; Andreas et al. 2012; Vickers et al. 2013).

The functional forms and coefficients for the wind speed and bulk stability dependencies in the simple model are determined from a large observational dataset including multiple experiments and aircraft covering a wide range of atmospheric conditions (Fig. 1). Based on the sign of the air–sea virtual potential temperature difference, conditions are unstable 57% of the time and stable 43% of the time. The wind speed ranges from 0.01 to 27.1 m s^{-1}.

2. Aircraft data

The aircraft dataset consists of over 5000 eddy-covariance measurements collected by four different aircraft in nine different experiments (Table 1). These data have recently been used in studies by Mahrt et al. (2012), Andreas et al. (2012), and Vickers et al. (2013), and additional information can be found in those studies and references therein.

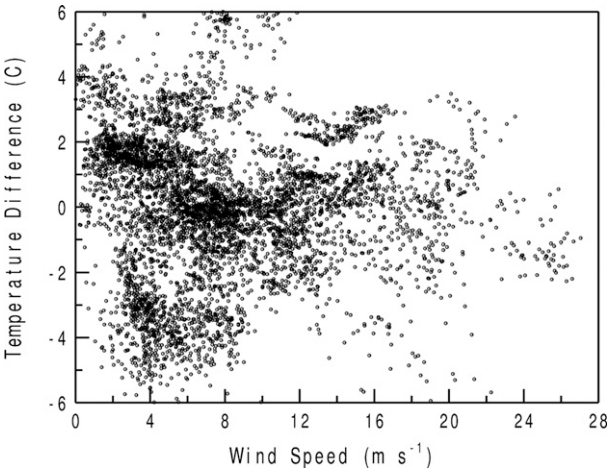

FIG. 1. The parameter space of the combined aircraft dataset (Table 1) for the temperature difference ($\theta_s - \theta_v$: the surface temperature minus the virtual potential temperature at height z) and the mean wind speed at height z. Each dot represents one 4-km-average data point with estimates of the mean flow and the fluxes.

The Twin Otter, C-130, and Electra used a five-port 20- or 25-Hz radome (gust probe) mounted on the nose of the aircraft to obtain the fast-response pressure measurements. The LongEZ used the Best Atmospheric Turbulence Probe (BAT), a 50-Hz, nine-port radome on a boom extending 2 m ahead of the nose and five wing widths in front of the canard (Crawford and Dobosy 1992; Garman et al. 2006). The basic principles for obtaining the 3D wind vector from fast-response aircraft measurements of pressure are given in Lenschow (1986). To calculate the true ground speed, all aircraft employed the global positioning system to correct the aircraft's inertial navigation (Khelif et al. 1999). The Twin Otter, Electra, and C-130 measured the sea surface radiative temperature with a Heitronics Infrarot Messtechnik GmbH Model KT 19.85; the LongEZ used an Everest Interscience, Inc., Model 4000.4GXL. Air temperature was measured using microbead thermistors. The LongEZ instrumentation is further described in Sun et al. (2001).

3. Methods

a. Flux calculations

To ensure consistency for the data collected by the different aircraft in different experiments, we obtained the fast-response data and applied identical screening procedures, quality control testing, and flux calculations to each dataset. The eddy-covariance fluxes, mean wind

TABLE 1. The aircraft datasets used in this study, where N is the number of flux estimates, U is the mean wind speed ($m\,s^{-1}$), U_{max} is the maximum wind speed ($m\,s^{-1}$), and u_* is the mean friction velocity ($m\,s^{-1}$). Information on these datasets can be found in Vickers et al. (2013), Andreas et al. (2012, 2015), Mahrt et al. (2012), and references therein. Sampling rates are 40, 25, 20, and 50 Hz for the Twin Otter, C-130, Electra, and LongEZ, respectively, and nominal ground speeds are 65, 100, 100, and 55 $m\,s^{-1}$ for the Twin Otter, C-130, Electra, and LongEZ, respectively. Here, CIRPAS is the Center for Interdisciplinary Remotely Piloted Aircraft Studies, NCAR is the National Center for Atmospheric Research, NOAA is the National Oceanic and Atmospheric Administration, CARMA is the Cloud-Aerosol Research in the Marine Atmosphere experiment, RED is the Rough Evaporation Duct experiment, POST is the Physics of Stratocumulus Top experiment, and CBLAST is the Coupled Boundary Layers and Air Sea Transfer experiment.

Aircraft, expt, date	N	U	U_{max}	u_*
CIRPAS Twin Otter, CARMA IV, Aug 2007	649	7.3	18.0	0.22
CIRPAS Twin Otter, Monterey, Apr 2008	592	11.2	18.1	0.38
CIRPAS Twin Otter, RED, Aug–Sep 2001	373	7.9	17.9	0.26
CIRPAS Twin Otter, POST, Jul–Aug 2008	189	8.4	13.8	0.27
NCAR C-130, GOTEX, Feb 2004	859	15.8	27.1	0.60
NCAR Electra, TOGA COARE, Nov 1992–Feb 1993	938	3.9	9.4	0.16
NOAA LongEZ, SHOWEX, Nov 1997	508	6.5	12.0	0.25
NOAA LongEZ, SHOWEX, Nov 1999	829	6.1	16.5	0.21
NOAA LongEZ, CBLAST, Jul–Aug 2001	760	5.3	9.2	0.15

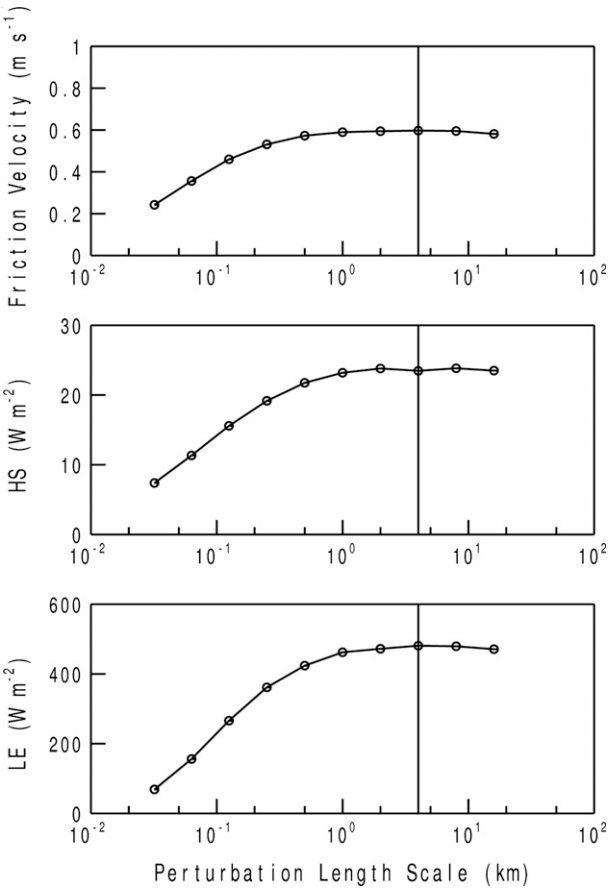

FIG. 2. Cumulative dependence of the flux on the spatial scale used to define the fluctuations for the friction velocity, sensible heat flux (HS), and LE. The vertical line denotes the constant 4-km window used to compute the fluxes in this study. The dependence shown here is a composite for flight 9 in GOTEX.

speed, temperature, and humidity are calculated from data collected during low-altitude (10–50 m) flight segments where aircraft altitude, roll, pitch, and heading fluctuations remained within prescribed limits. The fast-response measurements of the wind, temperature, and humidity that pass this first level of screening are then scanned by quality control software to identify suspected instrumental errors. The quality control procedure tests for the following manifestations of instrument problems: a high frequency of spikes, data outside a specified range, very large skewness, very small or large kurtosis, a large local Haar mean transform (discontinuity in the mean), and a local standard deviation outside a specified range. Flagged data are plotted for visual inspection, and data exhibiting implausible behavior are removed from further analysis.

For computing the eddy-covariance turbulence fluxes, we use a short 4-km window to reduce the impact of surface heterogeneity (changes in sea surface temperature). Multiresolution decomposition of the flux (Howell and Mahrt 1997; Vickers and Mahrt 2006) indicates that a 4-km window is more than sufficient to capture the largest eddies that contribute to the turbulence fluxes of momentum, heat, and moisture, even for the high wind speed and strong turbulence Gulf of Tehuantepec Experiment (GOTEX) data (Fig. 2). In fact, Fig. 2, sometimes called an ogive plot, shows that there is very little additional flux at scales exceeding 1 km. Mahrt et al. (2012) recently pointed out a similar scale dependence of the heat flux. Individual 4-km flux estimates do suffer from large random flux sampling errors; however, our multiresolution flux decomposition analysis indicates that they do not suffer from systematic errors due to using a window that is too small.

b. *Monin–Obukhov similarity theory and the Charnock relation*

The turbulence fluxes of momentum (M), sensible heat (H), and latent heat (LE) at the air–sea interface

are formulated in almost all atmospheric models using the following flux–gradient relationships:

$$M \equiv \rho u_*^2 = \rho C_d U^2, \tag{1}$$

$$H \equiv \rho c_p \overline{w'\theta'} = \rho c_p C_h U(\theta_s - \theta), \quad \text{and} \tag{2}$$

$$\mathrm{LE} \equiv \rho L_v \overline{w'q'} = \rho L_v C_q U(q_s - q). \tag{3}$$

Average wind speed U, potential temperature θ, and specific humidity q are evaluated at some height z above the surface; θ_s is the surface temperature; and q_s is the saturated specific humidity at the surface temperature. In our analysis, primes denote perturbations from a 4-km mean, and the overbar denotes 4-km averaging. In Eq. (1), u_* is the friction velocity.

The exchange coefficients are given by Monin–Obukhov similarity theory as (e.g., Garratt 1992)

$$C_d = \left[\frac{\kappa}{\ln(z/z_{\mathrm{om}}) - \psi_m}\right]^2, \tag{4}$$

$$C_h = \left[\frac{\kappa}{\ln(z/z_{\mathrm{om}}) - \psi_m}\right]\left[\frac{\kappa}{\ln(z/z_{\mathrm{oh}}) - \psi_h}\right], \quad \text{and} \tag{5}$$

$$C_q = \left[\frac{\kappa}{\ln(z/z_{\mathrm{om}}) - \psi_m}\right]\left[\frac{\kappa}{\ln(z/z_{\mathrm{oq}}) - \psi_q}\right], \tag{6}$$

where $\kappa = 0.4$ is the von Kármán constant; ψ_m, ψ_h, and ψ_q are the stability functions; and z_{om}, z_{oh}, and z_{oq} are the roughness lengths corresponding to transport of momentum, heat, and moisture, respectively. The stability functions in unstable conditions come directly from Paulson (1970), while the stability functions in stable conditions come from Panofsky and Dutton [(1984); Eq. (10) on p. 136 for momentum; and Eq. (14) on p. 147 for heat and moisture].

The aerodynamic roughness length in the Tropical Ocean and Global Atmosphere (TOGA) Coupled Ocean–Atmosphere Response Experiment (COARE) bulk flux scheme is given by

$$z_{\mathrm{om}} = \alpha u_*^2/g + 0.11\nu/u_*, \tag{7}$$

where α is the Charnock coefficient and ν is the kinematic viscosity of dry air (Charnock 1955; Smith 1988; Fairall et al. 1996). We use the usual value of $\alpha = 0.011$ [e.g., COARE, version 2.6; Fairall et al. (1996)]. The second term on the right side of Eq. (7) is the viscous or aerodynamically smooth flow term, which is important in weak winds (Kondo 1975). The roughness lengths for heat and moisture are specified as functions of the roughness Reynolds number after the surface-renewal theory of Liu et al. (1979). In version 3.0 of the COARE scheme (Fairall et al. 2003), the roughness lengths were found empirically and are slightly greater for wind speeds exceeding $10\,\mathrm{m\,s^{-1}}$ than in COARE 2.6, thus slightly increasing the modeled fluxes in strong winds.

c. *Model for u_* based on the 10-m neutral wind*

Andreas et al. (2012) proposed a formulation for the friction velocity in terms of the 10-m neutral wind, where their 10-m neutral wind is calculated as

$$U_{\mathrm{N10}} = U - (u_*/\kappa)\ln(z/10) + (u_*/\kappa)\psi_m(z/L). \tag{8}$$

This approach [see Eq. (2.1) in Andreas et al. (2012)] reduces the self-correlation between u_* and U_{N10}. Their linear formulation of u_* as a function of U_{N10} is based on the same nine aircraft datasets used in this study with the addition of processed (precalculated fluxes) datasets collected on towers, ships, and other aircraft. While there is no roughness length in their formulation, the method still relies on Monin–Obukhov similarity theory because the stability function ψ_m is a function of the Obukhov length L. The formulation must be solved iteratively because u_* is required to estimate U_{N10}, which is used to estimate u_*, and so on. The formulation of Andreas et al. (2012) has the desirable property that the 10-m neutral equivalent drag coefficient naturally rolls off at high wind speed and asymptotically approaches a constant value of 3.4×10^{-3}.

4. Results

In the simple model, the friction velocity is formulated as the product of functions of the mean wind speed and the mean bulk stability as

$$u_* = f(U)h(R_b), \tag{9}$$

where U is the wind speed and R_b is the bulk Richardson number,

$$R_b = \frac{(\theta_v - \theta_s)gz}{\theta_v U^2}, \tag{10}$$

where θ_v is the virtual potential temperature. The bulk Richardson number has been discussed extensively in the air–sea interaction literature (e.g., Deardorff 1968; Grachev and Fairall 1997). Unlike MOST, in the simple model, the measured wind speed is not adjusted based on height or stability; however, height is constrained to be between 10 and 50 m, corresponding to the height of our aircraft measurements. The functional forms and

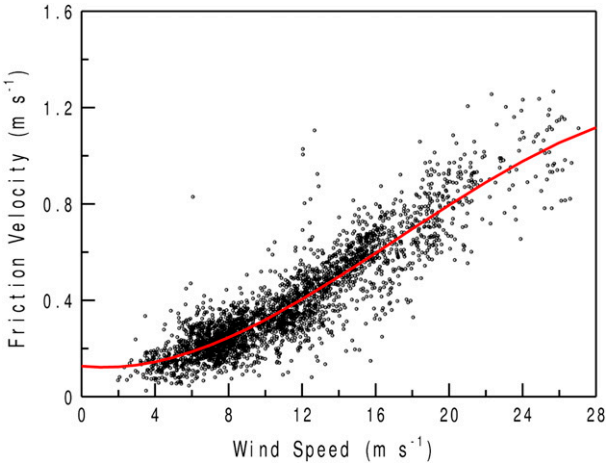

FIG. 3. The 4-km-average observations of the friction velocity and mean wind speed for the combined dataset for near-neutral conditions only, where the magnitude of $R_b < 0.02$. Aircraft height above the sea surface ranges from 10 to 50 m. The red curve is the least squares fit to a third-order polynomial [Eq. (11)].

coefficients in Eq. (9) will be determined from the combined dataset including all nine experiments (Table 1).

To obtain $f(U)$, we examine the wind speed dependence of the friction velocity for near-neutral cases only, where the magnitude of R_b is less than 0.02 and $h(R_b)$ is expected to be near unity. That is, we isolate the wind speed dependence by looking only at those data where bulk stability effects are thought to be relatively small. In all, 2948 data points, or 52% of the total data points, satisfy this near-neutral criterion. Based on visual inspection of the wind speed dependence of the friction velocity, we choose a third-order polynomial to describe the wind speed dependence of u_* in near-neutral flow (Fig. 3).

Multiple regression yields

$$f(U) = 0.17 - 0.019U + 0.0042U^2 - 8.410^{-5}U^3, \quad (11)$$

where $f(U)$ and U have units of meters per second. This third-order polynomial explains 83% of the variance of u_* with no adjustments for variation in height. The cubic fit is likely not valid for wind speeds in excess of 30 m s^{-1}; however, we do not have the data to test it.

Estimates of the uncertainty of the regression coefficients are developed using a random sampling scheme, where we sampled the full set of near-neutral data points randomly and did the regression analysis for each subset individually. Each of 20 such subsets has approximately one-half of the data. The standard deviation of the regression coefficients over the 20 runs is considered an estimate of the uncertainty. The mean and 95% confidence limits (± 2 standard deviations) for the four coefficients in Eq. (11) are, respectively, 0.17 $\pm$ 0.03, -0.019 ± 0.009, 0.0042 ± 0.0008, and $-8.4 \times 10^{-5} \pm 2.0 \times 10^{-5}$.

The polynomial fit described by Eq. (11) and shown in Fig. 3 handles the problematic weak wind case by maintaining nonzero friction velocity as the mean wind speed approaches zero. The friction velocity may actually vanish or become undefined with very weak winds or for winds following swells (Vickers and Mahrt 2010). Such cases can be found in the observations; however, imposing zero surface stress in a numerical model may not be appropriate because numerical models represent grid-box area-averaged fluxes, while collapsed turbulence is likely a local transient phenomenon where zero surface stress leads to flow acceleration and generation of turbulence (Vickers and Mahrt 2010).

This third-order polynomial based on the combined dataset [Eq. (11)] is also a reasonable representation of the wind speed dependence of the friction velocity in near-neutral conditions for each dataset individually (Fig. 4). It is encouraging that one formulation can describe all nine datasets individually and collectively. This fact suggests that wave state effects may be secondary to wind speed effects. Figure 4 also highlights the importance of having multiple datasets when the range of wind speeds for an individual dataset is small.

The bulk stability function is obtained from Eq. (9) as

$$h(R_b) = u_*/f(U), \quad (12)$$

where we use the combined dataset including all nine experiments and all the data, including where the magnitude of R_b exceeds 0.02 and stability effects are likely important. An approximate fit to the bulk stability dependence (Fig. 5) is

$$h(R_b) = (1 - 60R_b)^{0.1}; \quad R_b < 0 \quad \text{and} \quad (13)$$

$$h(R_b) = (1 + 60R_b)^{-0.2}; \quad R_b > 0. \quad (14)$$

Because we fitted the stability function by eye, the uncertainty analysis that we performed for $f(U)$ and the near-neutral data using the random sampling scheme is not possible for $h(R_b)$. Nevertheless, we could still evaluate how sensitive this function is to the coefficients. The stability function is not especially sensitive to the coefficient of 60 in Eqs. (13) and (14), since changing the coefficient by a factor of 2 (from 60 to 120 or from 60 to 30) changes the value of $h(R_b)$ by only about 10% for R_b of about -0.1 or $+0.1$. When R_b is ± 0.1, changing the exponent coefficient of 0.1 in Eq. (13) by a factor of 2 changes the value of $h(R_b)$ by about 20%, and changing the exponent coefficient of -0.2 in Eq. (14) by a factor of 2 changes $h(R_b)$ by about 25%.

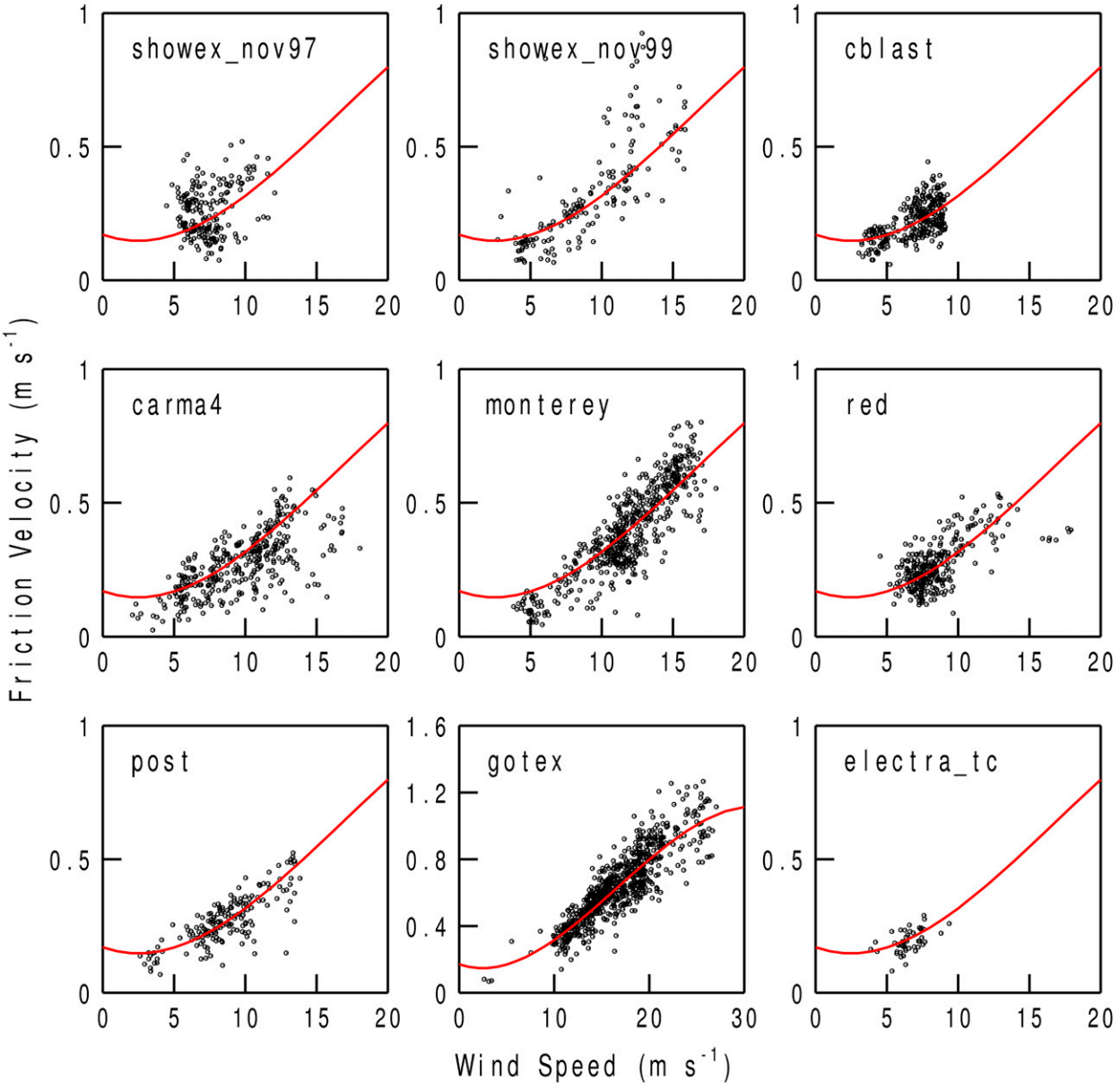

FIG. 4. The 4-km-average observations of the friction velocity as a function of mean wind speed for only near-neutral conditions for each individual dataset. Aircraft height above the sea surface ranged from 10 to 50 m. The red curves are the least squares fit to a third-order polynomial for the combined dataset including all nine experiments [Eq. (11) and Fig. 3]. The plot axes are the same for all panels except for GOTEX.

It is encouraging that the bulk Richardson number dependence is well behaved for strong stability. For strongly unstable conditions with $R_b = -0.1$, $h(R_b) = 1.2$. That is, u_* is 1.2 times u_* in near-neutral conditions for the same wind speed. For strongly stable conditions with $R_b = 0.1$, $h(R_b) = 0.7$. The stability function given by Eqs. (13) and (14) has a "long tail," meaning that it does not go to zero and totally destroy the turbulence even with very strong bulk stability, nor does it become unphysically large with very strong instability. For strong stability, $h(R_b)$ is not sensitive to small changes in R_b. We cannot comment on the validity if $h(R_b)$ outside the range $-0.1 < R_b < 0.1$, the limits of our data.

As found for $f(U)$, here we determine that a single formulation of $h(R_b)$ does a reasonable job of describing the datasets both individually and collectively (Fig. 6). Possible exceptions include the Shoaling Waves Experiment (SHOWEX) from November 1997 and TOGA COARE. Some of these differences may be related to errors in the bulk Richardson number due to difficulties

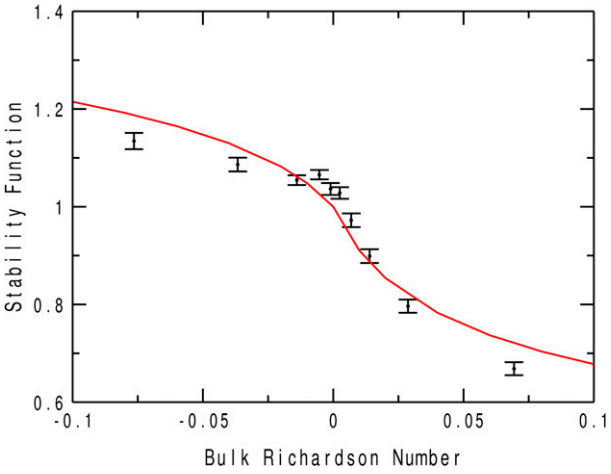

FIG. 5. The stability function [$h(R_b)$; see text] in the simple model based on the combined dataset. Each of the 10 bins contains 10% of the total number of 4-km data points. Error bars represent ± 1 standard error. The red curve is an approximate fit to the data given by Eqs. (13) and (14).

in measuring (calibrating) the surface radiative temperature (Mahrt et al. 2012). Recall that the stability function is typically a small correction to the wind speed dependence such that small errors in $h(R_b)$ may not be fatal when the goal is to estimate u_*.

While the model [Eq. (9)] is "empirical," we note that all models of turbulence and boundary layer processes are empirical to some degree because they have some coefficient or sets of coefficients that are based on observations. The physical basis for the formulation of the simple model is that we know from previous studies that stronger winds lead to stronger shear generation of turbulence and larger momentum transport in the presence of mean wind shear, and that stronger bulk stability leads to stronger buoyancy destruction of turbulence and relatively smaller momentum transport in the presence of mean wind shear.

a. Reproducing the observations

Figure 7 compares the friction velocities from the simple model and the COARE version-2.6 scheme with the observed friction velocities. Comparing how well the two models agree with the observations may not be fair to the COARE scheme because the simple model coefficients are tuned to the observations. On the other hand, recall that the simple model coefficients based on the combined nine experiments also describe reasonably well each of the individual experiments (Figs. 4 and 6). The fact that the simple model tends to fit all nine experiments individually and collectively indicates that it is not overly tuned to any single experiment and in fact may be fairly general. The differences in the squared correlation (R^2), the root-mean square (RMS), and the bias between the simple model and the observations and the COARE scheme and the observations are likely insignificant, suggesting that differences between the simple model and the COARE scheme are small relative to the observational uncertainty (Fig. 7). Note that the COARE scheme has approximately 70 empirical parameters while the simple model has only 10.

The formulation of the friction velocity in terms of the 10-m neutral wind proposed by Andreas et al. (2012) yields estimates of the friction velocity that are similar to those from the simple model and the COARE scheme (not shown). Differences in the R^2, RMS, and bias values between the Andreas model and the COARE scheme are small.

b. Dependence on measurement height

The COARE model u_* residuals (model minus observed) bin averaged by measurement height are near zero for the lowest measurement heights and negative for the measurement heights exceeding about 30 m (Fig. 8). The simple model residuals are also near zero for the lowest measurement heights; however, they are positive for the higher measurement heights. Positive residuals found for higher measurement heights are consistent with an underestimate of the observed u_* because of significant vertical flux divergence, possibly associated with shallow boundary layers. It is not clear why the COARE residuals would be systematically negative for higher measurement heights.

The simple model residuals are closer to zero than the COARE residuals for all measurement heights. Thus, even though we might expect a strong height dependence for the simple model residuals because there is no normalization of wind speed to a reference level, we actually find that the COARE scheme yields a stronger height dependence. The stronger height dependence implies that Monin–Obukhov similarity is not working, and may do more harm than good. Note, however, that the bin-averaged u_* residuals in Fig. 8 are small, not exceeding more than a few hundredths of a meter per second.

c. Distribution of residuals

The probability distributions of relative model residuals for the simple model and the COARE scheme for each dataset individually are shown in Figs. 9 and 10, respectively. We generally find good results for both models and all datasets in that small residuals occur more frequently, and large residuals occur more rarely. A possible exception is the Electra TOGA COARE dataset, where the simple model systematically overpredicts u_* while the COARE scheme tends to underpredict u_* with large scatter. Recall that we obtained the

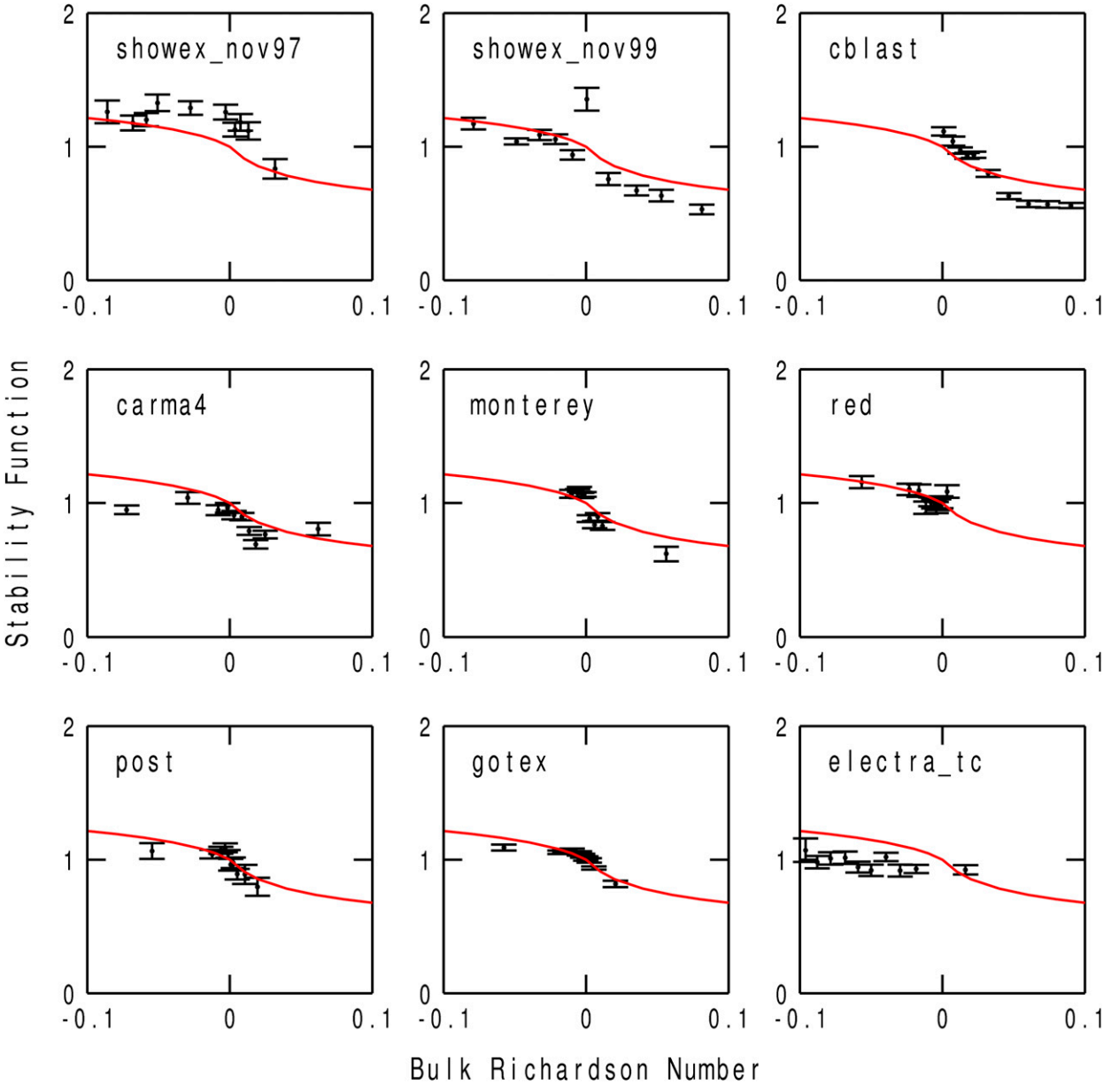

FIG. 6. The stability function for each individual dataset. Each of the 10 bins contains 10% of the total number of 4-km data points. Error bars represent ±1 standard error. The red curves are the least squares fit based on the combined dataset that includes all nine experiments [Eqs. (13) and (14); Fig. 5].

raw aircraft data and did our own data analysis such that it is almost certain that our set of observed TOGA COARE fluxes are different than those fluxes based on ship data used to construct the COARE algorithm. The TOGA COARE dataset has the weakest winds of all the datasets and therefore has large relative uncertainty in the calculated fluxes.

The narrowest distribution of relative residuals, indicating that the model almost always performs well, is found for the C-130 GOTEX dataset, which also has the strongest wind speeds. In terms of the relative error, both models perform better in strong winds than in weak winds. This could be due, in part, to the larger uncertainty in the calculated fluxes in weak winds.

We have demonstrated that the simple model can provide a reasonable description of the friction velocity for all nine datasets individually and collectively. That is, the functional forms and the coefficients in $f(U)$ and $h(R_b)$ are not especially sensitive to which experiments are used to evaluate the coefficients. This result implies

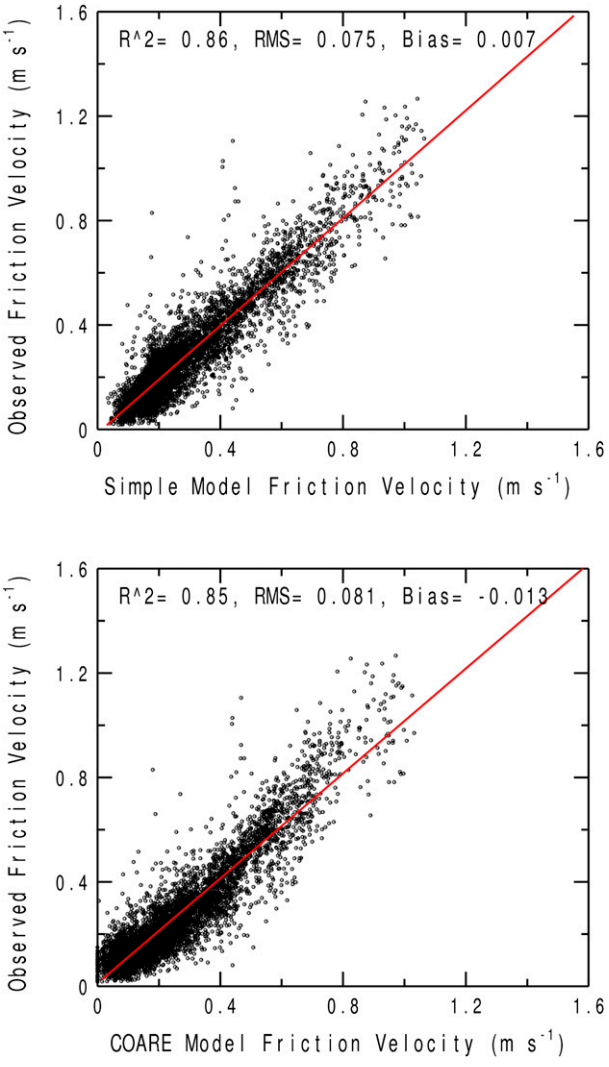

FIG. 7. The observed friction velocity as a function of the friction velocity from (top) the simple model and (bottom) the full COARE scheme (version 2.6) with Monin–Obukhov similarity and the Charnock relation. The red lines are from least squares linear regression.

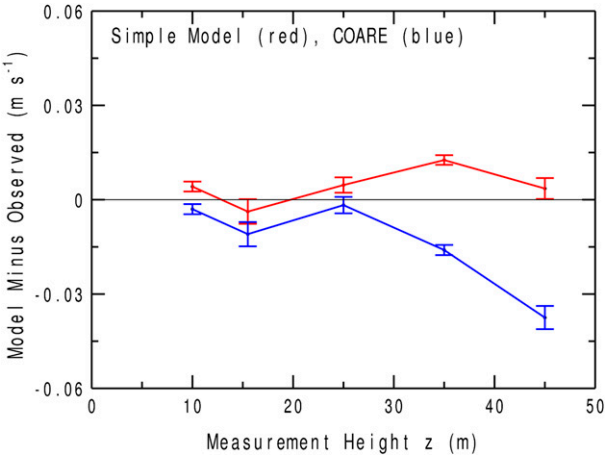

FIG. 8. The measurement height dependence of the model friction velocity residuals for the simple model and the COARE scheme. Error bars represent ±1 standard error. The numbers of 4-km data points in each bin (left to right) are 116, 612, 1112, 2178, and 679.

that the formulations of $f(U)$ and $h(R_b)$ may be fairly general; however, it is unclear exactly how general. The model does not include any information on wave state; and therefore variations in wave state, possibly associated with swell and the direction of the waves in relation to the direction of the wind, may contribute to scatter and unexplained variance.

d. Independent model evaluation

In this section, we compare the simple model predictions of u_* to the observations from three independent eddy-covariance datasets: ship data from the Fronts and Atlantic Storm Track Experiment (FASTEX; Persson et al. 2005); aircraft data from the Greenland Flow Distortion Experiment (GFDEX; Petersen and Renfrew 2009); and offshore platform tower data from the Humidity Exchange Over the Sea (HEXOS; DeCosmo 1991). These three datasets were recently analyzed by Andreas et al. (2012, 2015). We did not obtain the raw data for these datasets and, thus, could not apply our standard quality control analysis and flux computation. Values of the measurement height, mean wind speed, virtual potential temperature, and sea surface temperature were input into the simple model to predict the friction velocity; the results are shown in Fig. 11.

The variance of the observed u_* explained by the simple model is large: ranging from 83% for FASTEX, to 88% for GFDEX, and to 92% for HEXOS. These high R^2 values are due in part to the lack of weak wind data, where the observed fluxes are most uncertain. The average u_* values for these three datasets are 0.51, 0.75, and 0.48 m s^{-1} for FASTEX, GFDEX, and HEXOS, respectively. In addition, the stability correction is relatively small because the wind speeds are strong, and thus the uncertainty associated with the stability function becomes less important. The nondimensional slopes from linear regression are 1.13, 0.87, and 1.16 for FASTEX, GFDEX, and HEXOS, respectively (Fig. 11). The mean biases in u_* (the mean modeled value minus the mean observed) are −0.03, 0.02, and −0.07 m s^{-1} for FASTEX, GFDEX, and HEXOS, respectively. The mean relative biases in u_* (the mean modeled value minus the mean observed normalized by the mean) are −6%, 2%, and −15% for FASTEX, GFDEX, and HEXOS, respectively.

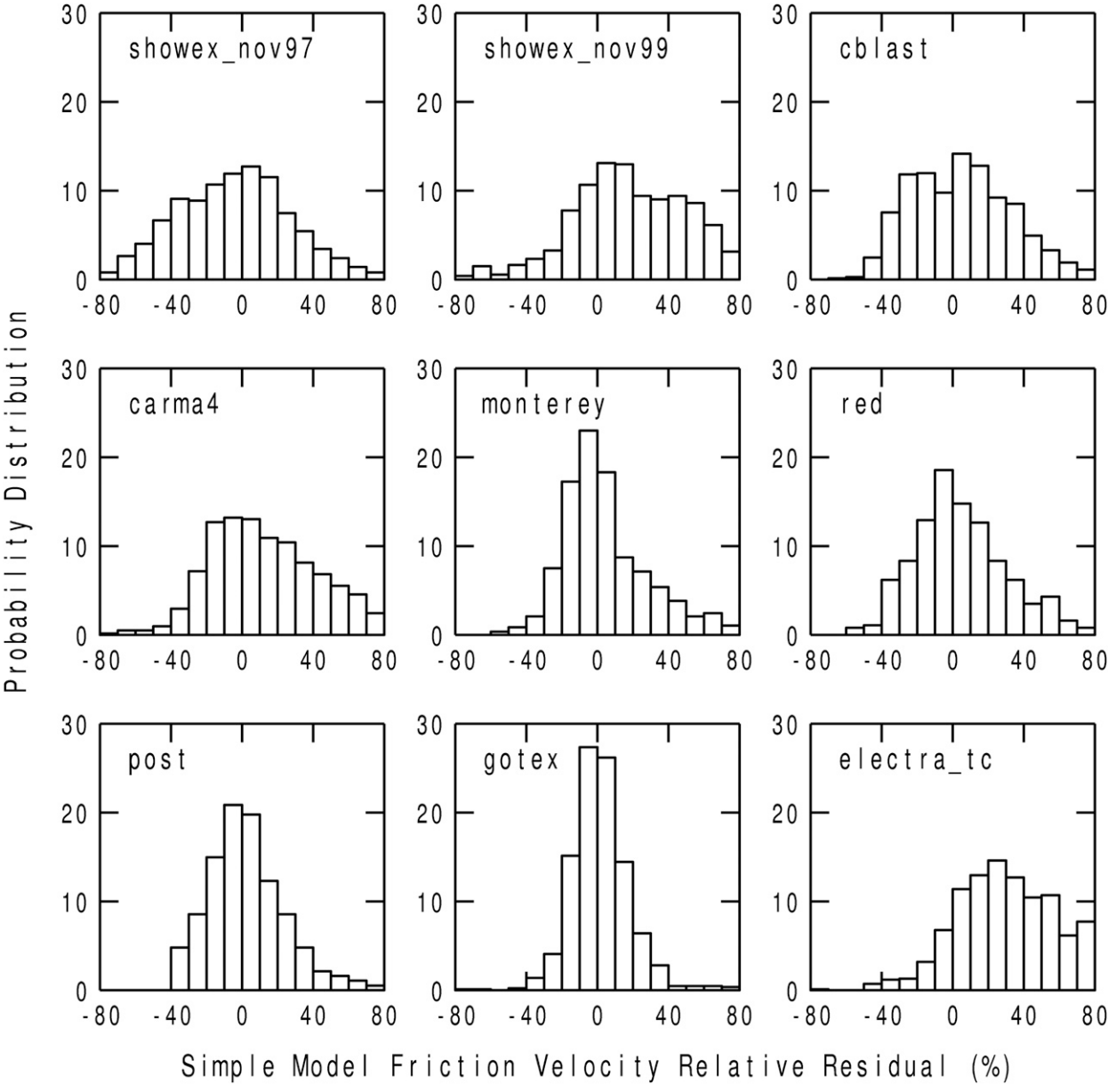

FIG. 9. Distribution (%) of the simple model relative residuals in the friction velocity (simple model minus observed divided by observed) for each individual dataset.

This analysis demonstrates that the simple model may be of general use for predicting the friction velocity.

5. Conclusions

Our simple model is based on a third-order polynomial that predicts the friction velocity from the wind speed in near-neutral conditions. An additional function based on the bulk Richardson number applies a correction for stability. The simple model does not require an estimate of the Obukhov length or the aerodynamic roughness length, both of which are subject to large uncertainty; and it does not require iteration. The model coefficients are tuned using data from four different aircraft in nine different experiments comprising 5000 observations.

We do not correct the independent variable, wind speed, for height or stability but instead use the measured value of the mean wind speed in the third-order polynomial. The height of the measured wind speed is constrained to be between 10 and 50 m above the sea surface. We do not standardize the wind speed to a constant height, say 10 m, as is typically done in observational

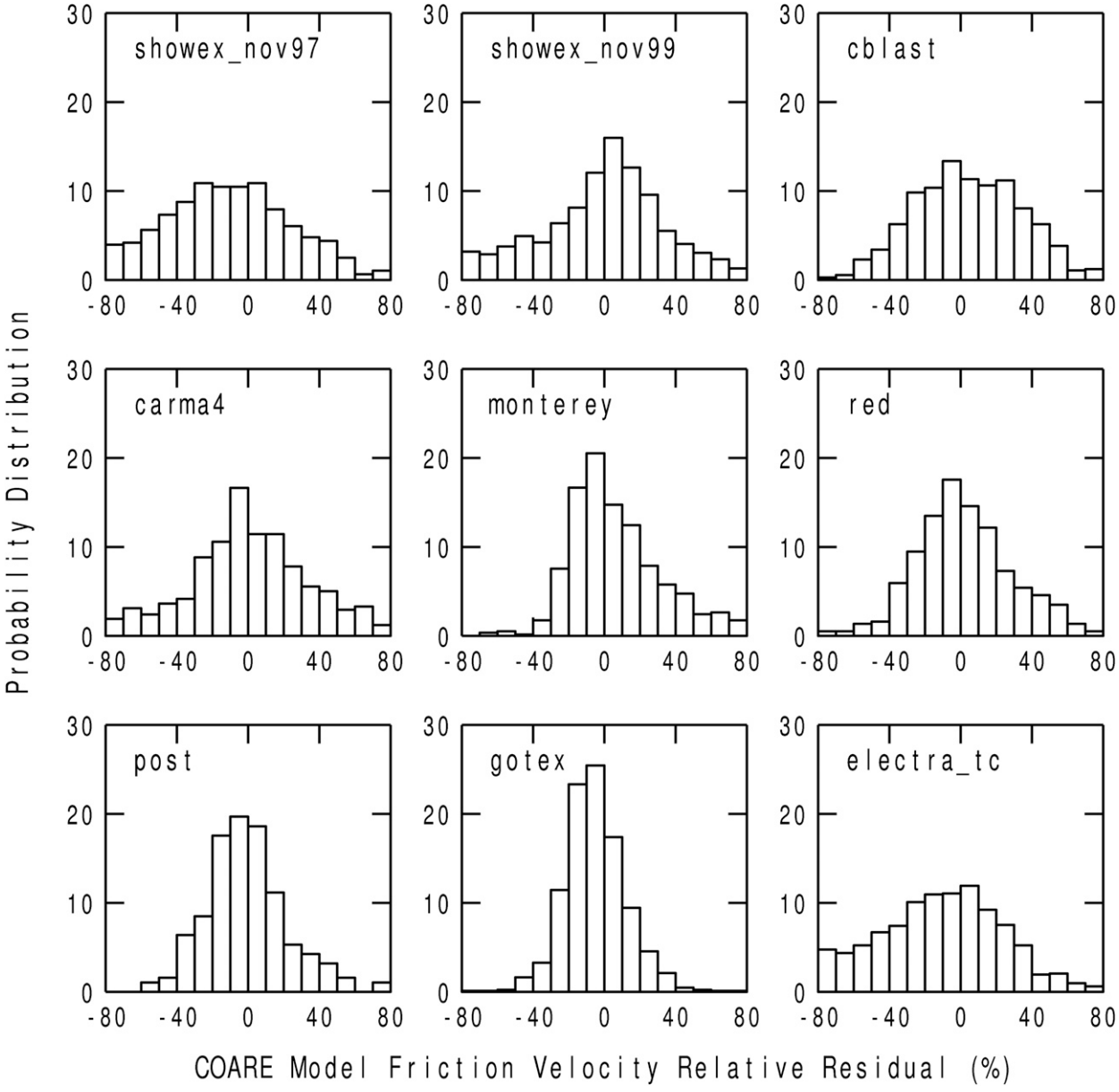

FIG. 10. Distribution of the COARE scheme residuals in the friction velocity (COARE scheme minus observed divided by observed) for each individual dataset.

studies because doing so would require introducing the quantity that we are estimating, friction velocity, into the independent variable, wind speed.

The friction velocities from both the simple model and the COARE scheme, which is based on a full implementation of Monin–Obukhov similarity theory and the Charnock relation, compare well to the observations. The simple model with coefficients tuned to a combination dataset also reasonably reproduces the observed friction velocities for each of the nine experiments individually. Similar close agreement was found between the simple model and a recently published formulation of the friction velocity based on a linear dependence on the 10-m neutral equivalent wind. In addition, the simple model was effective in predicting the friction velocity for three independent datasets. This work shows that discarding the complexity of Monin–Obukhov similarity theory and avoiding the large uncertainty in estimating the Obukhov length and the roughness length can lead to a credible model for the friction velocity for most situations.

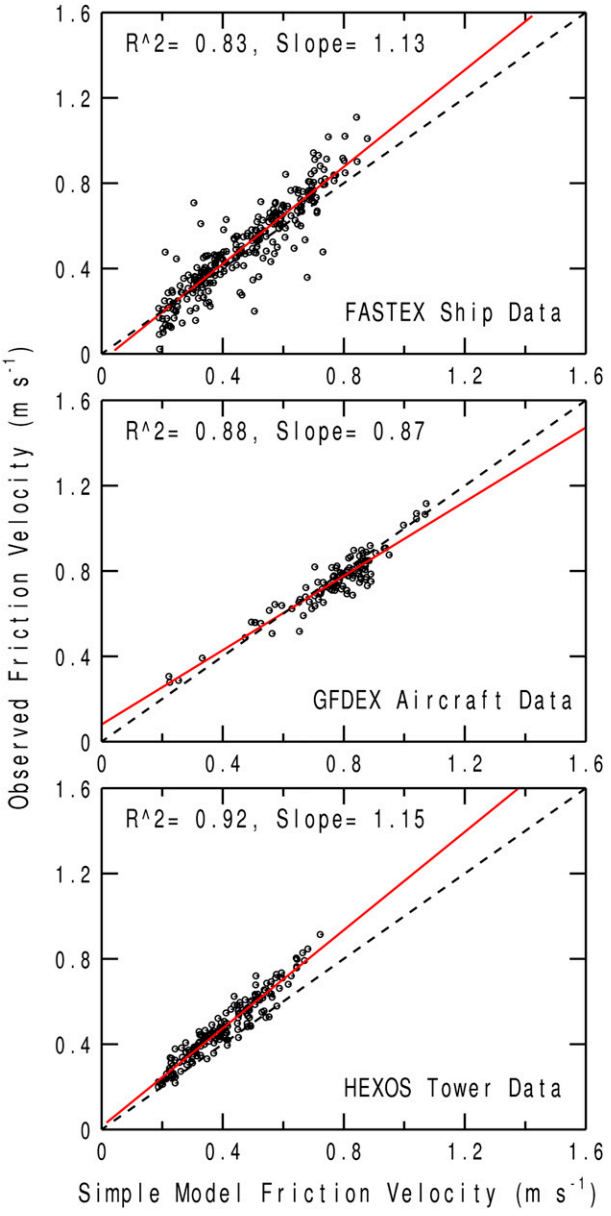

FIG. 11. The observed friction velocity vs the friction velocity predicted by the simple model for three independent datasets: FASTEX, GFDEX, and HEXOS. The red lines are from linear regression, and the dotted line is the 1-to-1 line. The numbers of data points are 263, 108, and 173 for FASTEX, GFDEX, and HEXOS, respectively.

Acknowledgments. We thank the three reviewers and the many dedicated scientists who collected and made available the data. The U.S. Office of Naval Research supported this work with Award N00014-11-1-0073 to NorthWest Research Associates. The Office of Naval Research also supported ELA with Award N00014-12-C-0290.

REFERENCES

Andreas, E. L, and B. B. Hicks, 2002: Comments on "Critical test of the validity of Monin–Obukhov similarity during convective conditions." *J. Atmos. Sci.,* **59,** 2605–2607, doi:10.1175/1520-0469(2002)059<2605:COCTOT>2.0.CO;2.

——, L. Mahrt, and D. Vickers, 2012: A new drag relation for aerodynamically rough flow over the ocean. *J. Atmos. Sci.,* **69,** 2520–2537, doi:10.1175/JAS-D-11-0312.1.

——, ——, and ——, 2015: An improved bulk air–sea flux algorithm, including spray-mediated transfer. *Quart. J. Roy. Meteor. Soc.,* doi:10.1002/qj.2424, in press.

Baas, P., G. J. Steeneveld, B. J. H. Van De Wiel, and A. A. M. Holtslag, 2006: Exploring self-correlation in flux–gradient relationships for stably stratified conditions. *J. Atmos. Sci.,* **63,** 3045–3054, doi:10.1175/JAS3778.1.

Charnock, H., 1955: Wind stress over a water surface. *Quart. J. Roy. Meteor. Soc.,* **81,** 639–640, doi:10.1002/qj.49708135027.

Crawford, T. L., and R. J. Dobosy, 1992: A sensitive fast-response probe to measure turbulence and heat flux from any air plane. *Bound.-Layer Meteor.,* **59,** 257–278, doi:10.1007/BF00119816.

Deardorff, J. W., 1968: Dependence of air–sea transfer coefficients on bulk stability. *J. Geophys. Res.,* **73,** 2549–2557, doi:10.1029/JB073i008p02549.

DeCosmo, J., 1991: Air–sea exchange of momentum, heat and water vapor over whitecap sea states. Ph.D. dissertation, University of Washington, 212 pp.

Fairall, C. W., E. F. Bradley, D. P. Rogers, J. B. Edson, and G. S. Young, 1996: Bulk parameterization of air-sea fluxes for Tropical Ocean-Global Atmosphere Coupled-Ocean Atmosphere Response Experiment. *J. Geophys. Res.,* **101,** 3747–3764, doi:10.1029/95JC03205.

——, ——, J. E. Hare, A. A. Grachev, and J. B. Edson, 2003: Bulk parameterization of air–sea fluxes: Updates and verification for the COARE algorithm. *J. Climate,* **16,** 571–591, doi:10.1175/1520-0442(2003)016<0571:BPOASF>2.0.CO;2.

Garman, K. E., and Coauthors, 2006: An airborne and wind tunnel evaluation of a wind turbulence measurement system for aircraft-based flux measurements. *J. Atmos. Oceanic Technol.,* **23,** 1696–1708, doi:10.1175/JTECH1940.1.

Garratt, J. R., 1992: *The Atmospheric Boundary Layer.* Cambridge University Press, 316 pp.

Grachev, A. A., and C. W. Fairall, 1997: Dependence of the Monin–Obukhov stability parameter on the bulk Richardson number over the ocean. *J. Appl. Meteor.,* **36,** 406–414, doi:10.1175/1520-0450(1997)036<0406:DOTMOS>2.0.CO;2.

Hicks, B. B., 1978: Some limitations of dimensional analysis and power laws. *Bound.-Layer Meteor.,* **14,** 567–569, doi:10.1007/BF00121895.

Howell, J., and L. Mahrt, 1997: Multiresolution flux decomposition. *Bound.-Layer Meteor.,* **83,** 117–137, doi:10.1023/A:1000210427798.

Kenney, B. C., 1982: Beware of spurious self-correlation! *Water Resour. Res.,* **18,** 1041–1048, doi:10.1029/WR018i004p01041.

Khelif, D., S. P. Burns, and C. A. Friehe, 1999: Improved wind measurements on research aircraft. *J. Atmos. Oceanic Technol.,* **16,** 860–875, doi:10.1175/1520-0426(1999)016<0860:IWMORA>2.0.CO;2.

Klipp, C. L., and L. Mahrt, 2004: Flux-gradient relationship, self-correlation and intermittency in the stable boundary layer. *Quart. J. Roy. Meteor. Soc.,* **130,** 2087–2103, doi:10.1256/qj.03.161.

Kondo, J., 1975: Air-sea bulk transfer coefficients in diabatic conditions. *Bound.-Layer Meteor.,* **9,** 91–112, doi:10.1007/BF00232256.

Lenschow, D. H., 1986: Aircraft measurements in the boundary layer. *Probing the Atmospheric Boundary Layer,* D. H. Lenschow, Ed., Amer. Meteor. Soc., 39–55.

Liu, W. T., K. B. Katsaros, and J. A. Businger, 1979: Bulk parameterization of the air–sea exchange of heat and water vapor including the molecular constraints at the interface. *J. Atmos. Sci.,* **36,** 1722–1735, doi:10.1175/1520-0469(1979)036<1722:BPOASE>2.0.CO;2.

Mahrt, L., D. Vickers, J. Sun, T. Crawford, J. Crescenti, and P. Fredrickson, 2001: Surface stress in offshore flow and quasi-frictional decoupling. *J. Geophys. Res.,* **106,** 20 629–20 640, doi:10.1029/2000JD000159.

——, ——, E. L Andreas, and D. Khelif, 2012: Sensible heat flux in near-neutral conditions over the sea. *J. Phys. Oceanogr.,* **42,** 1134–1142, doi:10.1175/JPO-D-11-0186.1.

Panofsky, H. A., and J. A. Dutton, 1984: *Atmospheric Turbulence: Models and Methods for Engineering Applications*. John Wiley and Sons, 397 pp.

Paulson, C. A., 1970: The mathematical representation of wind speed and temperature profiles in the unstable atmospheric surface layer. *J. Appl. Meteor.,* **9,** 857–861, doi:10.1175/1520-0450(1970)009<0857:TMROWS>2.0.CO;2.

Persson, P. O. G., J. E. Hare, C. W. Fairall, and W. D. Otto, 2005: Air-sea interaction processes in warm and cold sectors of extratropical cyclonic storms observed during FASTEX. *Quart. J. Roy. Meteor. Soc.,* **131,** 877–912, doi:10.1256/qj.03.181.

Petersen, G. N., and I. A. Renfrew, 2009: Aircraft-based observations of air-sea fluxes over Denmark Strait and the Irminger Sea during high wind speed conditions. *Quart. J. Roy. Meteor. Soc.,* **135,** 2030–2045, doi:10.1002/qj.355.

Smith, S. D., 1988: Coefficients for sea surface wind stress, heat flux, and wind profiles as a function of wind speed and temperature. *J. Geophys. Res.,* **93,** 15 467–15 472, doi:10.1029/JC093iC12p15467.

Sun, J., D. Vandemark, L. Mahrt, D. Vickers, T. Crawford, and C. Vogel, 2001: Momentum transfer over the coastal zone. *J. Geophys. Res.,* **106,** 12 437–12 488, doi:10.1029/2000JD900696.

Vickers, D., and L. Mahrt, 2006: A solution for flux contamination by mesoscale motions with very weak turbulence. *Bound.-Layer Meteor.,* **118,** 431–447, doi:10.1007/s10546-005-9003-y.

——, and ——, 2010: Sea-surface roughness lengths in the mid-latitude coastal zone. *Quart. J. Roy. Meteor. Soc.* **136,** 1089–1093, doi:10.1002/qj.617.

——, ——, and E. L Andreas, 2013: Estimates of the 10-m neutral sea surface drag coefficient from aircraft eddy-covariance measurements. *J. Phys. Oceanogr.,* **43,** 301–310, doi:10.1175/JPO-D-12-0101.1.